



Electrical Contacts in SOI MEMS Using Aerosol Jet Printing

Citation

Khorrarnadel, B., Torkkeli, A., & Mäntysalo, M. (2017). Electrical Contacts in SOI MEMS Using Aerosol Jet Printing. IEEE Journal of the Electron Devices Society, 6, 34-40. <https://doi.org/10.1109/JEDS.2017.2764498>

Year

2017

Version

Publisher's PDF (version of record)

Link to publication

[TUTCRIS Portal \(http://www.tut.fi/tutcris\)](http://www.tut.fi/tutcris)

Published in

IEEE Journal of the Electron Devices Society

DOI

[10.1109/JEDS.2017.2764498](https://doi.org/10.1109/JEDS.2017.2764498)

Take down policy

If you believe that this document breaches copyright, please contact cris.tau@tuni.fi, and we will remove access to the work immediately and investigate your claim.

Electrical Contacts in SOI MEMS Using Aerosol Jet Printing

Behnam Khorramdel,^{1*} Altti Torkkeli,² and Matti Mäntyselä¹

¹Department of Electronics and Communications Engineering, Tampere University of Technology, Tampere 33720, Finland

²Murata Electronics Oy, Vantaa, Finland

Abstract In this study, an additive method to make electrical contacts in SOI MEMS devices with aerosol jet printing is introduced. Small grooves were etched to the frame of MEMS accelerometer in the same step with the active structure release. Aluminum ink was jetted to the trenches in wafer-level to bridge the device layer to the handle wafer with the minimum amount of material. After subsequent annealing ohmic contacts between p-type device layer and p-type handle silicon were verified by I-V measurements. The via resistance less than 4 Ω per via is measured. The method demonstrated in this work provides simple and low-cost approach for SOI handle contact where additional packaging of wafer process steps can be avoided.

Keywords: microelectromechanical systems (MEMS), silicon on insulator (SOI), inkjet printing, aerosol jet printing, additive manufacturing

* **Corresponding Author:** behnam.khorramdel@tut.fi, T. +358 50 301 3907

1. INTRODUCTION

Single crystal Silicon-on-Insulator (SOI) is versatile material for various microelectromechanical system (MEMS) devices like accelerometers, gyroscopes, pressure sensors, optics and timing devices [1]–[3]. SOI provides several advantages compared to polycrystalline silicon, which is another widely used structural material [3], such as excellent material properties of single crystal silicon, no built-in stress, and wide variety of device layer thicknesses. It can also be integrated with pre-fabricated cavities to avoid perforation for release etching and to eliminate stiction to substrate [2], [4].

SOI MEMS suffers, however, from the difficulty of forming electrical contacts to the handle wafer. As solution, both packaging and wafer-level technologies have been used. Packaging methods include connecting the handle wafer in the metal bottom of the cavity using conductive chip adhesive or die bonding with eutectic metal [5] or additional wire bonding in the handle wafer back side [6]. These solutions may degrade device performance due to package related stresses or increase size of the package. Wafer-level method adds several process steps including etching small contact holes through the device layer and the buried oxide, depositing polysilicon or metal into the holes to make bridge over

the buried oxide [7], and removal of the filling material by chemical-mechanical planarization (CMP) or etching in order to maintain wafer surface properties suitable for subsequent processing and wafer encapsulation. As a result, device processing cost is highly increased and in worst case also the device layer thickness uniformity and device performance are degraded.

Inkjet printing as an additive and digital fabrication method has already been investigated for the dielectric filling and increasing the I/O density for rigid interposers [8], metallization of through silicon vias (TSVs) [9]–[14] and high-aspect ratio TSVs [15] in order to have fewer process steps and less waste material compared to the conventional methods. Accordingly, this paper reports a new method of forming the contacts between device layer and handle wafer by jetting the nano-metal ink using aerosol jet printing (AJP). This non-contact deposition method has been reported for several applications like printing of transistors [16]–[20], multi-layer ceramic capacitors [21], strain gauges [22], electrode arrays [23], solar cells [24]–[30], flexible displays [31], circuits [32], biological sensors [33], [34], solid oxide fuel cells [35], [36], sensors and actuators [37], RF [38], [39], and interconnects [40]. Since this method can be used to deposit material selectively without any wet or lithography step, it can be made for

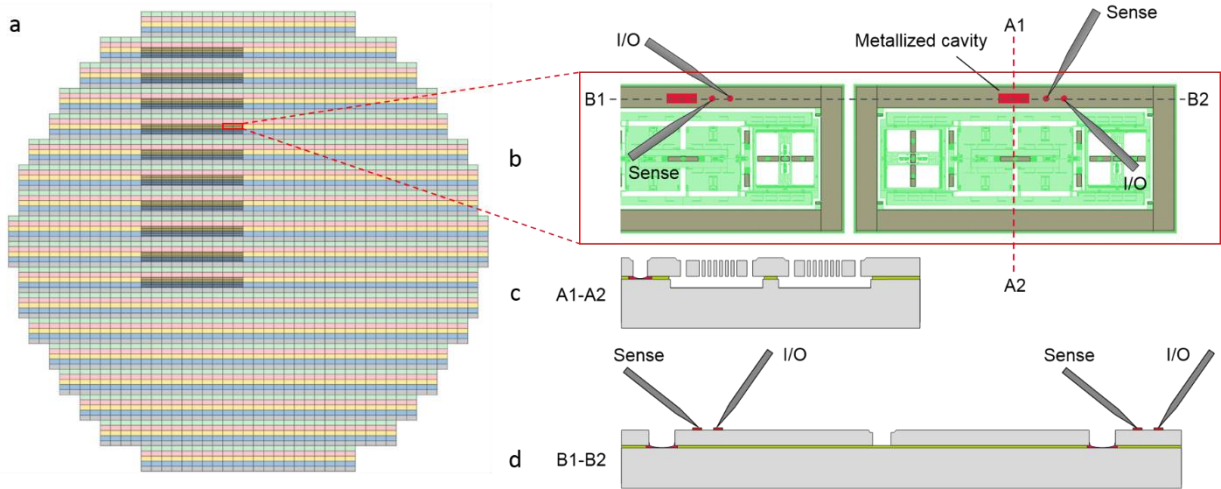


Figure 1. Schematic of (a) whole device layer with metallized frames highlighted, (b) 4-point resistance measurement setup from top view, (c) vertical x-sectional view over device frame and (d) horizontal x-sectional view over two adjacent device frames used for electrical measurement.

released MEMS structures before packaging. Since contact holes are formed in same process steps with the active structures, the number of additional process steps is very low, comprising only application of nano-metal ink and thermal treatment for ink drying and sintering.

2. MATERIALS AND METHODS

A. Materials

Aluminum ink (Al-IS1000) from Applied Nanotech, Austin, TX formulated for aerosol jet printing with viscosity of 80-120 cP was used for metallization of the cavities. Preliminary tests showed that for better coverage and reducing the overspray effect, the ink needed to be diluted. Therefore, 20.5 g of the original ink was diluted by 16.5 g of pure ethylene glycol. The ink manufacturer has reported sheet resistance less than 10 m Ω /sq which is function of firing temperature [41].

The test devices in this work are MEMS accelerometers with additional rectangular or oblong shape via cavities provided by Murata Electronics, Vantaa, Finland. The device layer (50 μ m) is floating on top of the 6-inch handle wafer (625 μ m) covered with buried oxide layer (2 μ m) as shown in Figure 1c&d. The test wafer was processed ready for wafer-level capping so that the movable structures were released by deep reactive ion etching (DRIE) followed by HF vapor etch.

B. Metallization/fabrication process

Aerosol Jet 300 CE with pneumatic atomizer manufactured by Optomec, Albuquerque, NM was used to deposit the Al ink into the cavities to make the

electrical connection between the device layer and handle wafer.

As marked in Figure 1a, ten sections including ten frames with oblong cavities and ten frames with rectangular cavities (totally 200 cavities) with the size of 60 μ m \times 240 μ m were selected to be metallized with the nano-Al ink. For every section, a different set of printing parameters was selected for the metallization. This design for the printing experiments was done in order to study the effect of printing parameters and geometry of the cavities on the quality of the interconnects and the electrical performance. Table 1 summarizes the printing parameters that were used for metallization of all ten sections; including: substrate temperature, sheath atomizing flow rate, atomizing flow rate and exhaust flow rate. As reported in the Table 1, the most important change between the sections has been the jetting or dispensing time. We also see that the nozzle has been mostly in center of the cavities except two sections (9 and 10). In these two cases, the ink is deposited while nozzle was moving along 90 μ m path.

Other than metallization of the cavities, as shown in Figure 2 three pads were printed just beside all the cavities to enable the electrical measurements and verifying the ohmic connection between the frames.

After the printing, first the wafer was placed in the oven with 100 $^{\circ}$ C for 30 minutes to dry the printed aluminum ink. Next, according to the ink manufacturer's sintering recipe the wafer was placed in a high temperature oven already heated up to 800 $^{\circ}$ C for two minutes in air.

There is also possibility to use annealing temperatures as low as 550 $^{\circ}$ C. However, in this study high-

temperature sintering was selected for two reasons: 1. it is recommended to use a forming gas atmosphere (4% H₂ in balance N₂) for low-temperature sintering but there was no access to an oven with such atmosphere during the experimental phase, and 2. according to the study by H. Platt et al. [42], [43], higher annealing temperatures (for the same Al ink used for this study) can result in lower contact resistivity. For instance, contact resistance of 80 mΩ-cm² in case of annealing at 550 °C can drop to 20 mΩ-cm² in case of annealing at 800 °C. Annealing at 800 °C, which is more than Al melting point (660 °C) and Al-Si eutectic point (577 °C), can increase the diffusion in the interface of the Al and the Si wafer that results in a lower contact resistivity. Same authors have reported that in higher annealing temperature (800 °C), there is no significant contribution from the printed Al and measured resistances is mainly coming from the contact.

Table 1. Printing parameters used for the metallization of both oblong and rectangular cavities of all sections. TP: substrate temperature (°C), Sh: sheath atomizing flow rate (ccm), Atom: atomizing flow rate (ccm) and Exh: exhaust flow rate (ccm).

Section	TP	Sh	Atom	Exh	Time	Shooting spot
1	20	90	1035	1000	2	Center
2	20	90	1035	1000	1	Center
3	20	90	1035	1000	1.5	Center
4	20	90	1035	1000	2.5	Center
5	20	90	1036	1000	3	Center
6	20	90	1036	1000	10	Center
7	20	90	1036	1000	7	Center
8	20	90	1036	1000	5	Center
9	20	90	1036	1000	5	motion 90 μm
10	20	90	1036	1000	2.5	motion 90 μm

C. Characterization methods

Olympus BX51 optical microscope was used for testing the geometry of the metal plugs after the sintering.

In order to measure resistance values and remove the errors, four-point resistance measurement (using printed Al pads) was performed using a Keithley 2400 sourcemeter for all 180 pairs of frames (oblong and rectangular). Figure 1b&d are representing the setup used for four-point resistance measurement. Device under test included two adjacent frames. This means that the measured resistance includes two via resistances.

After testing the electrical performance, sections 1, 3, 4 (short printing time), 6, 7 (longer printing time) and 9 (longer printing time + nozzle motion) were selected for cross-sectional analysis in order to understand how printing time or the amount of the printed material could effect on the resistance.

Precision cross section system (Gatan Ilion+TM Advantage) was used for the final preparation of the cross-sections of the metallized cavities using broad ion beam (BIB) to introduce least possible damage to the samples. The cross-sections were milled using 6 kV argon ions and a ~ 100 μm thick layer was removed.

Jeol JSM-6335F field emission Scanning Electron Microscope (SEM) was used for the cross-sectional characterization of the metallized and non-metallized cavities.

3. RESULTS AND DISCUSSION

Top-down optical micrographs, showed that longer holding time or printing more material inside the cavities could result in more uniform coverage at the bottom of the cavities, compared with non-uniform and central coverage in case of shorter printing times. This difference could be observed by for example comparing section 3 with 1 second printing and section 6 with 10 seconds printing (Figure 2). Ink splashes on the wafer surface are a problem for wafer bonding which need to be eliminated by further development. The amount of extra ink over-sprayed on the wafer surface could be controlled by shorter printing time, changing the viscosity of the ink, gas flow rate and better nozzles. Printing parameters for each section could be found from Table 1.

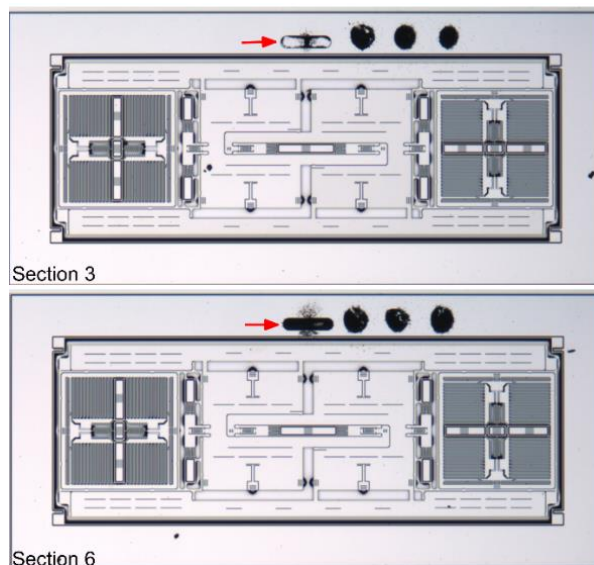


Figure 2. Top-down view of the metallized oblong cavities (pointed by arrows) after the sintering for sections 3 and 6. Three printed spots on the right side of the cavities are for electrical characterization.

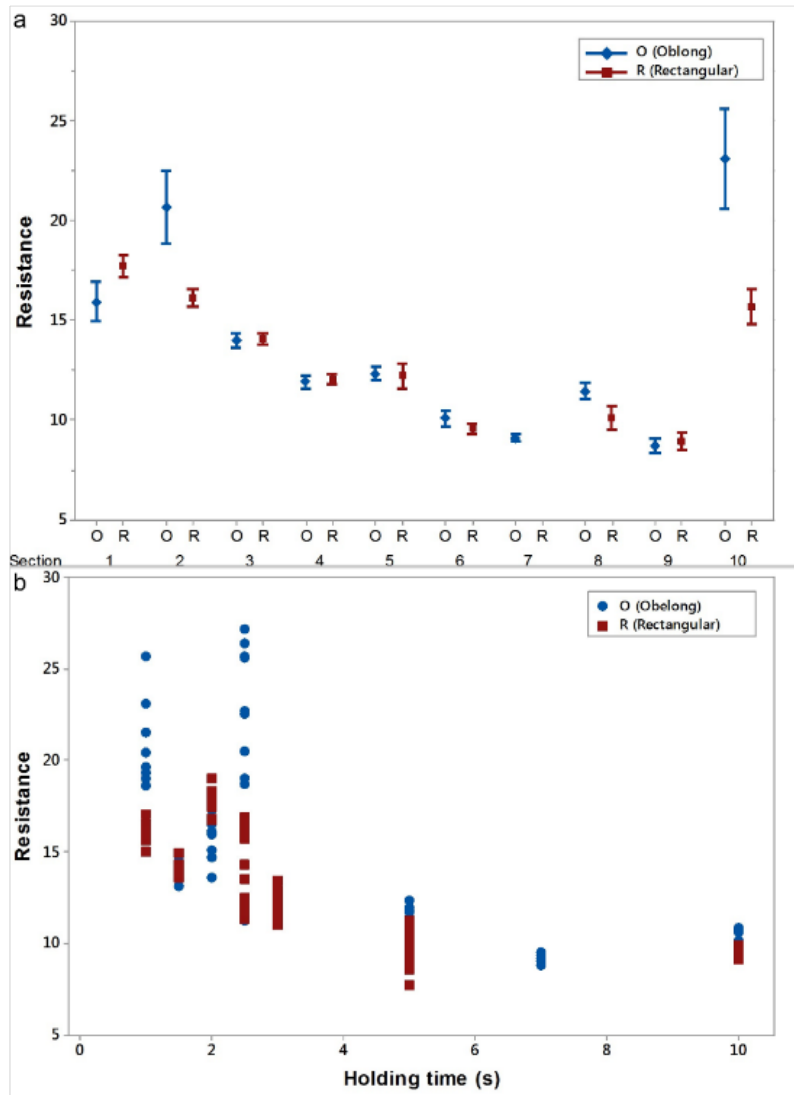


Figure 3. (a) The result of the four-point via resistance measurements for sections 1-10. Blue lines with diamonds represent oblong and red lines with square represent rectangular. The bars presents 95% confidence intervals. (b) The resistance as a function of holding time. Blue circles represent oblong and red squares represent rectangular.

In this study, quite large cavities ($60 \times 240 \mu\text{m}$) were designed to match the resolution of the available tool (close to $50 \mu\text{m}$). The cavities were placed inside the sealing frame (width $200 \mu\text{m}$) of the MEMS accelerometer and since they act as non-continuities in the frame it is desirable to keep their size as small as possible to ensure proper hermetic sealing. State-of-the-art aerosol jet printers are capable for feature sizes down to $10 \mu\text{m}$ with $\pm 10\%$ and placement accuracy of $\pm 1 \mu\text{m}$ [44]. Effect of independently increasing process variables on printed line width is studied in [45]. It is reported that increasing the focusing ratio (sheath gas

flow rate divided by carrier gas flow rate), decreasing the nozzle diameter and increasing the stage speed can result in narrower lines. Such performance would enable using smaller cavities, down to $20 \mu\text{m}$ or below which is small enough not to cause any negative effect in the reliability of the sealing frame.

Due to a continuous scaling trend towards smaller devices and dimensions, even smaller vias are needed. Since the ink-jet technology is under strong development, it is possible that smaller contacts become available in the future so that they approach the diameters of the polysilicon or metal filled SOI vias

(<10 μm). In addition, electro-hydrodynamic printing (EHD), with the droplet size less than 1 μm , is another alternative to deposit the nano-metal inks inside the very small via cavities even in the range of less than 10 μm when the appropriate material is available [46]. Furthermore, metallization of very thin vias with the size of 23 μm is demonstrated in [15].

It must be noticed that the actual design area for such vias is larger than the nominal mask diameter because margins for CMP planarization non-idealities like dishing and erosion or etch mask overlap must be included, especially when the vias are placed in the sealing frame or in another bondable structure. Therefore it is reasonable to expect that after some technical development the ink-jet approach can provide cost-effective alternative for current via contacts, at least in SOI MEMS applications with thick device layers and fragile structures.

Figure 3a is representing the overall result of the four-point via resistance measurements for sections 1-10. Figure shows the average and 95% confidential intervals of each section presented in Table 1. As seen from the results, the smallest resistance is 7.7 Ω and highest resistance is 27.2 Ω , which means that the via resistance is less than 4 Ω per via. According to [43], the resistivity of a printed line with the width of 100 μm and thickness of 10 μm on glass after appropriate sintering is 10 $\mu\Omega\text{-cm}$ which is ~ 6 times of resistivity of bulk aluminum. It can be seen that oblong shows little bit wider variation especially in section 1, 2, and 10. These three cases have small holding time. Small holding time results in poorer connections, which explains the most of the variation. Based on the data, however, we would not make the claim that oblong gives poorer results. Variation is more related to the amount of material and process variation.

Figure 3b shows the resistance as a function of holding time. As you can see from this image, the resistance decreases as a function of holding time. After 5 seconds, the resistance stabilizes. There is minor increase in resistance from 7 seconds (section 7) to 10 seconds (section 6), but this is order of normal process variation (couple of Ohms).

Figure 4 shows the SEM cross-sectional image of a non-metallized frame (a), bird view of a partially metallized frame from section 4 with 2.5 seconds printing (b), partially metallized oblong frame from section 3 with 1.5 seconds printing (c) and partially metallized oblong frame from section 7 with 7 seconds printing (d). It should be noted that the cross-sections are not exactly from the center of the frames because of limitations for the sample preparation.

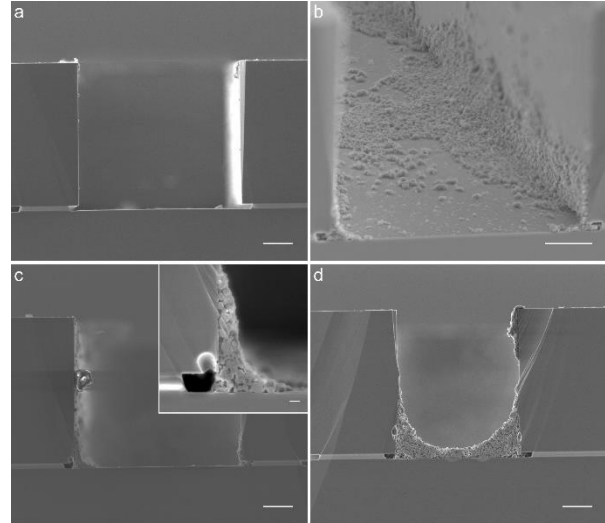


Figure 4. SEM cross-sectional image of (a) a non-metallized frame, (b) bird view of a partially metallized frame with 2.5 seconds printing, (c) partially metallized oblong frame with 1.5 seconds printing and (d) partially metallized oblong frame with 7 seconds printing. Scale bars: 10 μm .

Because of the aerosol behavior and a relatively viscous ink (even after the dilution) we observed that the distribution of the ink after jetting the material in the center of the cavities, was not uniform at the bottom and the ink was not penetrated uniformly inside the very right and left bottom corners. However, this presented approach for the partial metallization was still beneficial for making a good conductive bridge between the device layer and the handle wafer. It was also found that longer printing time or printing more material could make a better coverage and improve the conductivity even more.

When the printing time is longer (Figure 4d), there is more possibility to have better and more uniform coverage at the very corners of the cavity. This will make a better connection. Short printing time leads to non-uniform coverage, and therefore, poor connection at the bottom of the cavities as demonstrated in Figure 4b and c. It seems that when the printing time is long enough to cover better the corners (e.g. ≥ 5 seconds), an optimum distribution of the ink can result in a bit lower resistance. For example, enough amount of material (5 seconds printing) is dispensed into the sections 8 and 9 but dispensing with a 90 μm motion of the nozzle has resulted a more optimum distribution and lower resistance. It could be argued that a critical printing time (5 seconds) could be a point that the connection to the handle wafer is made all around the bottom of the cavities and contact resistance stabilizes. This argument is based on this fact that other parameters like focusing

ratio, substrate temperature, nozzle diameter and stage speed have all been kept fixed.

4. CONCLUSIONS

In this work, aerosol jet printing was realized as a feasible solution to make the bridge between the device layer and the handle wafer over the buried oxide in between. It was found that printing more nano-metal ink inside the cavities (≥ 5 seconds) could result in a lower resistance between the device frames because of the better coverage. The via resistance less than 4Ω per via was reached. However, printing much less material (ex. 1.5 seconds) could still result in a very good electrical performance. The via geometry (oblong or rectangular) didn't have remarkable difference in resistance. Printing time was the most important factor to decrease the resistance verified by cross-sectional images. It was also realized that jetting the ink in the center of the cavities would be more beneficial.

It should also be noted that in case of MEMS devices built on n++ wafers, piezo inkjet printing could also be used to deposit available inkjettable Au inks inside the cavities with good geometry and no ink splashes on the wafer surface. This approach was not used in this work since the Au ink was not able to make the ohmic connection in the case of using p+ silicon.

ACKNOWLEDGEMENTS

This work is supported by ENIAC-JU Project Prominent grant No. 324189 and Tekes grant No. 40336/12. M. Mäntysalo is supported by Academy of Finland grant Nos. 288945 and 294119.

The authors would like to acknowledge Murata Electronics for providing the wafers needed for this research work. We would also like to thank Jere Manni from Top Analytica, Finland for making the cross-sections of the metallized vias using a broad ion beam technique and Laurent Seronveaux from Sirris, Belgium for performing the metallization process using the aerosol jet printer. Authors would like to thank Heikki Kuisma in Murata Electronics for helpful discussion and guidance and Kaisa Nera in Murata Electronics for designing the mask for the via cavities.

REFERENCES

- [1] J. Kiihamäki, "Fabrication of SOI micromechanical devices," VTT Publications 559, 2005.
- [2] F. Assaderaghi, "SOI and Engineered-SOI, ideal platforms for building MEMS," in *2013 IEEE SOI-3D-Subthreshold Microelectronics Technology Unified Conference (S3S)*, 2013, pp. 1–2.
- [3] R. Ghodssi and P. Lin, Eds., *MEMS Materials and Processes Handbook*, vol. 1. Boston, MA: Springer US, 2011.
- [4] J. Karttunen, J. Mäkinen, and M. Tilli, "Intelligent silicon substrates for a shorter microsystem design cycle," in *Integration Issues of Miniaturized Systems-MOMS, MOEMS, ICS and Electronic Components (SSI), 2008 2nd European Conference & Exhibition on*, 2008, pp. 1–3.
- [5] M. Gad-el-Hak, "MEMS: design and fabrication," 2006.
- [6] M. J. Thompson and J. Seeger, "Microelectromechanical system device with internal direct electric coupling," 2016.
- [7] P. Lin, R. M. Boyssel, M. Boyssel, M. Winters, W. Hawkins, J. Kubby, P. Gulvin, J. Diehl, K. Feinberg, K. German, L. Herko, N. Jia, J. Ma, J. Meyers, P. Nystrom, and Y. R. Wang, "Multi-user hybrid process platform for mems devices using silicon-on-insulator wafers," in *18th IEEE International Conference on Micro Electro Mechanical Systems, 2005. MEMS 2005.*, pp. 516–519.
- [8] B. Khorramdel, J. Liljeholm, M.-M. Laurila, T. Lammi, G. Mårtensson, T. Ebefors, F. Niklaus, and M. Mäntysalo, "Inkjet printing technology for increasing the I/O density of 3D TSV interposers," *Microsystems Nanoeng.*, vol. 3, p. 17002, Apr. 2017.
- [9] A. Rathjen, Y. Bergmann, and K. Krüger, "Feasibility Study: Inkjet Filling of Through Silicon Vias (TSV)," in *NIP & Digital Fabrication Conference*, 2012, pp. 456–460.
- [10] B. Khorramdel and M. Mäntysalo, "Inkjet filling of TSVs with silver nanoparticle ink," in *Proceedings of the 5th Electronics System-Integration Technology Conference (ESTC)*, 2014, pp. 1–5.
- [11] B. Khorramdel and M. Mäntysalo, "Fabrication and electrical characterization of partially metallized vias fabricated by inkjet," *J. Micromechanics Microengineering*, vol. 26, no. 4, p. 45017, Apr. 2016.
- [12] K. Eiroma and H. Viljanen, "Application of inkjet printing for 3D integration," in *NIP & Digital Fabrication Conference*, 2015, pp. 195–200.

- [13] N. Quack, J. Sadie, V. Subramanian, and M. C. Wu, "Through Silicon Vias and thermocompression bonding using inkjet-printed gold nanoparticles for heterogeneous MEMS integration," in *2013 Transducers & Eurosensors XXVII: The 17th International Conference on Solid-State Sensors, Actuators and Microsystems (TRANSDUCERS & EUROSENSORS XXVII)*, 2013, pp. 834–837.
- [14] J. Sadie, N. Quack, M. C. Wu, and V. Subramanian, "Droplet-on-demand Inkjet-filled Through-silicon Vias (TSVs) as a Pathway to Cost-Efficient Chip Stacking," in *46th International Symposium on Microelectronics*, 2013, pp. 866–871.
- [15] B. Khorramdel, M. M. Laurila, and M. Mantysalo, "Metallization of high density TSVs using super inkjet technology," in *2015 IEEE 65th Electronic Components and Technology Conference (ECTC)*, 2015, pp. 41–45.
- [16] D. Braga, N. C. Erickson, M. J. Renn, R. J. Holmes, and C. D. Frisbie, "High-Transconductance Organic Thin-Film Electrochemical Transistors for Driving Low-Voltage Red-Green-Blue Active Matrix Organic Light-Emitting Devices," *Adv. Funct. Mater.*, vol. 22, no. 8, pp. 1623–1631, Apr. 2012.
- [17] J. H. Cho, J. Lee, Y. Xia, B. Kim, Y. He, M. J. Renn, T. P. Lodge, and C. Daniel Frisbie, "Printable ion-gel gate dielectrics for low-voltage polymer thin-film transistors on plastic," *Nat. Mater.*, vol. 7, no. 11, pp. 900–906, Nov. 2008.
- [18] Y. Xia, W. Zhang, M. Ha, J. H. Cho, M. J. Renn, C. H. Kim, and C. D. Frisbie, "Printed Sub-2 V Gel-Electrolyte-Gated Polymer Transistors and Circuits," *Adv. Funct. Mater.*, vol. 20, no. 4, pp. 587–594, Feb. 2010.
- [19] C. S. Jones, X. Lu, M. Renn, M. Stroder, and W.-S. Shih, "Aerosol-jet-printed, high-speed, flexible thin-film transistor made using single-walled carbon nanotube solution," *Microelectron. Eng.*, vol. 87, no. 3, pp. 434–437, Mar. 2010.
- [20] J. Zhao, Y. Gao, J. Lin, Z. Chen, and Z. Cui, "Printed thin-film transistors with functionalized single-walled carbon nanotube inks," *J. Mater. Chem.*, vol. 22, no. 5, pp. 2051–2056, Jan. 2012.
- [21] C. E. Folgar, C. Suchicital, and S. Priya, "Solution-based aerosol deposition process for synthesis of multilayer structures," *Mater. Lett.*, vol. 65, no. 9, pp. 1302–1307, May 2011.
- [22] M. Maiwald, C. Werner, V. Zoellmer, and M. Busse, "INKtelligent printed strain gauges," *Procedia Chem.*, vol. 1, no. 1, pp. 907–910, Sep. 2009.
- [23] A. Lesch, D. Momotenko, F. Cortés-Salazar, I. Wirth, U. M. Tefashe, F. Meiners, B. Vaske, H. H. Girault, and G. Wittstock, "Fabrication of soft gold microelectrode arrays as probes for scanning electrochemical microscopy," *J. Electroanal. Chem.*, vol. 666, pp. 52–61, Feb. 2012.
- [24] A. Kalio, M. Leibinger, A. Filipovic, K. Krüger, M. Glatthaar, and J. Wilde, "Development of lead-free silver ink for front contact metallization," *Sol. Energy Mater. Sol. Cells*, vol. 106, pp. 51–54, Nov. 2012.
- [25] A. Kalio, A. Richter, M. Hörteis, and S. W. Glunz, "METALLIZATION OF N-TYPE SILICON SOLAR CELLS USING FINE LINE PRINTING TECHNIQUES," *Energy Procedia*, vol. 8, pp. 571–576, 2011.
- [26] M. Hörteis and S. W. Glunz, "Fine line printed silicon solar cells exceeding 20% efficiency," *Prog. Photovoltaics Res. Appl.*, vol. 16, no. 7, pp. 555–560, Nov. 2008.
- [27] C. Yang, E. Zhou, S. Miyanishi, K. Hashimoto, and K. Tajima, "Preparation of Active Layers in Polymer Solar Cells by Aerosol Jet Printing," *ACS Appl. Mater. Interfaces*, vol. 3, no. 10, pp. 4053–4058, Oct. 2011.
- [28] A. Mette, P. L. Richter, M. Hörteis, and S. W. Glunz, "Metal aerosol jet printing for solar cell metallization," *Prog. Photovoltaics Res. Appl.*, vol. 15, no. 7, pp. 621–627, Nov. 2007.
- [29] P. Kopola, B. Zimmermann, A. Filipovic, H.-F. Schleiermacher, J. Greulich, S. Rousu, J. Hast, R. Myllylä, and U. Würfel, "Aerosol jet printed grid for ITO-free inverted organic solar cells," *Sol. Energy Mater. Sol. Cells*, vol. 107, pp. 252–258, Dec. 2012.
- [30] A. Ebong and N. Chen, "Metallization of crystalline silicon solar cells: A review," in *High Capacity Optical Networks and Emerging/Enabling Technologies*, 2012, pp. 102–109.
- [31] M. O'Reilly and J. Leal, "Jetting your way to fine-pitch 3D interconnects," *Chip Scale Review*, vol. 14, no. 5, pp. 18–21, 2010.
- [32] M. Ha, Y. Xia, A. A. Green, W. Zhang, M. J. Renn, C. H. Kim, M. C. Hersam, and C. D. Frisbie, "Printed, Sub-3V Digital Circuits on

- Plastic from Aqueous Carbon Nanotube Inks,” *ACS Nano*, vol. 4, no. 8, pp. 4388–4395, Aug. 2010.
- [33] I. Grunwald, E. Groth, I. Wirth, J. Schumacher, M. Maiwald, V. Zoellmer, and M. Busse, “Surface biofunctionalization and production of miniaturized sensor structures using aerosol printing technologies,” *Biofabrication*, vol. 2, no. 1, p. 14106, Mar. 2010.
- [34] S. Roy, “Fabrication of micro- and nano-structured materials using mask-less processes,” *J. Phys. D. Appl. Phys.*, vol. 40, no. 22, p. R413, 2007.
- [35] A. M. Sukeshini, P. Gardner, F. Meisenkothen, T. Jenkins, R. Miller, M. Rottmayer, and T. L. Reitz, “Aerosol Jet Printing and Microstructure of SOFC Electrolyte and Cathode Layers,” in *ECS Transactions*, 2011, vol. 35, no. 1, pp. 2151–2160.
- [36] A. M. Sukeshini, T. Jenkins, P. Gardner, R. M. Miller, and T. L. Reitz, “Investigation of Aerosol Jet Deposition Parameters for Printing SOFC Layers,” in *ASME 2010 8th International Fuel Cell Science, Engineering and Technology Conference: Volume 1*, 2010, pp. 325–332.
- [37] M. Landgraf, S. Reitelshofer, J. Franke, and M. Hedges, “Aerosol jet printing and lightweight power electronics for dielectric elastomer actuators,” in *2013 3rd International Electric Drives Production Conference (EDPC)*, 2013, pp. 1–7.
- [38] F. Cai, Y. Chang, K. Wang, W. T. Khan, S. Pavlidis, and J. Papapolymerou, “High resolution aerosol jet printing of D- band printed transmission lines on flexible LCP substrate,” in *2014 IEEE MTT-S International Microwave Symposium (IMS2014)*, 2014, pp. 1–3.
- [39] R. C. Roberts and N. C. Tien, “Multilayer passive RF microfabrication using jet-printed au nanoparticle ink and aerosol-deposited dielectric,” in *2013 Transducers & Eurosensors XXVII: The 17th International Conference on Solid-State Sensors, Actuators and Microsystems (TRANSDUCERS & EUROSENSORS XXVII)*, 2013, pp. 178–181.
- [40] Sungchul Joo and D. F. Baldwin, “Interfacial adhesion of nano-particle silver interconnects for electronics packaging application,” in *2008 58th Electronic Components and Technology Conference*, 2008, pp. 1417–1423.
- [41] “Al-IS1000 Spec and Application Sheet,” *Applied Nanotech, Inc.* [Online]. Available: <http://www.appliednanotech.net/>. [Accessed: 02-Aug-2017].
- [42] H. A. S. Platt, Y. Li, J. P. Novak, and M. F. A. M. van Hest, “Non-contact printed aluminum for metallization of Si photovoltaics,” *Thin Solid Films*, vol. 556, pp. 525–528, Apr. 2014.
- [43] H. A. S. Platt, Y. Li, J. P. Novak, and M. F. A. M. van Hest, “Non-contact printed aluminum metallization of Si photovoltaic devices,” in *2012 38th IEEE Photovoltaic Specialists Conference*, 2012, pp. 002244–002246.
- [44] B. King and M. Renn, “Aerosol Jet direct write printing for mil-aero electronic applications,” in *Palo Alto Colloquia, Lockheed Martin*, 2009.
- [45] A. Mahajan, C. D. Frisbie, and L. F. Francis, “Optimization of Aerosol Jet Printing for High-Resolution, High-Aspect Ratio Silver Lines,” *ACS Appl. Mater. Interfaces*, vol. 5, no. 11, pp. 4856–4864, Jun. 2013.
- [46] M. Mashayekhi, L. Winchester, L. Evans, T. Pease, M.-M. Laurila, M. Mantysalo, S. Ogier, L. Teres, and J. Carrabina, “Evaluation of Aerosol, Superfine Inkjet, and Photolithography Printing Techniques for Metallization of Application Specific Printed Electronic Circuits,” *IEEE Trans. Electron Devices*, vol. PP, no. 99, pp. 1–8, 2016.



Behnam Khorramdel received his M.Sc. (Tech) degree in Materials Science from Tampere University of Technology, Tampere, Finland in 2013. He is currently pursuing his doctoral studies with Tampere University of Technology, Tampere, Finland.



Dr. Altti Torkkeli received his M.Sc. and D.Sc. (Tech) degrees in Electrical engineering in Helsinki University of Technology, Finland in 1994 and 2003, respectively. From 1994 until 2003 he worked as research scientist in VTT Technical Research Centre of Finland with various MEMS device and process research topics including optical MEMS, microphones, pressure sensors and microfluidics. He joined Murata Electronics (former VTI Technologies) in 2003 and since then he has been working with MEMS process and platform development in different positions. He is currently Sr. Manager in New MEMS Technology Development with interest in new MEMS device concepts and manufacturing technologies.



Dr. Matii Mäntysalo received his M.Sc. and D.Sc. (Tech) degrees in electrical engineering in Tampere University of Technology, Tampere, Finland in 2004 and 2008, respectively.

He is an Associate Professor in Electronics materials and manufacturing in Tampere University of Technology, received Academy research fellow grant from Academy of Finland, and has awarded with Adjunct Professor in Digital fabrication in

Tampere University of Technology. Mäntysalo has led the Printable Electronics Research Group at TUT since 2008. He was a visiting scientist in iPack Vinn Excellence Center, School of information and Communication Technology, KTH Royal Institute of Technology, Stockholm, Sweden, from 2011 to 2012.

His research interests include printed electronics materials, fabrication processes, stretchable electronics, and especially integration of printed electronics with silicon-based technology (hybrid systems). Mäntysalo has more than 100 international journal and conference articles. He has served IEEE CMPT, IEC TC119 Printed electronics standardization, and Organic Electronics Association.